Catal Lett (2015) 145:1301–1306
DOI 10.1007/s10562-015-1517-4

Bio-template Route for the Facile Fabrication of TiO_2@*Bacillus subtilis* Composite Particles and Their Application for the Degradation of Rhodamine B

Chao Yan[1] · Diejing Feng[1] · Yunjie Jiang[1] · Xiaoying An[1] · Linjing Ye[1] · Weisheng Guan[1] · Bo Bai[2]

Received: 4 January 2015 / Accepted: 8 March 2015 / Published online: 18 March 2015

Abstract The *Bacillus subtilis* was used to synthesize the TiO_2@*Bacillus subtilis* composite particles via a single-step strategy based on electrostatic interaction driving self-assembling heterocoagulation. Such materials had a rod-shaped microstructure with uniform size (1.4 ± 0.1 μm in length; 450 ± 50 nm in width), and the removal ratio of rhodamine B was approximately 89 %.

Graphical Abstract

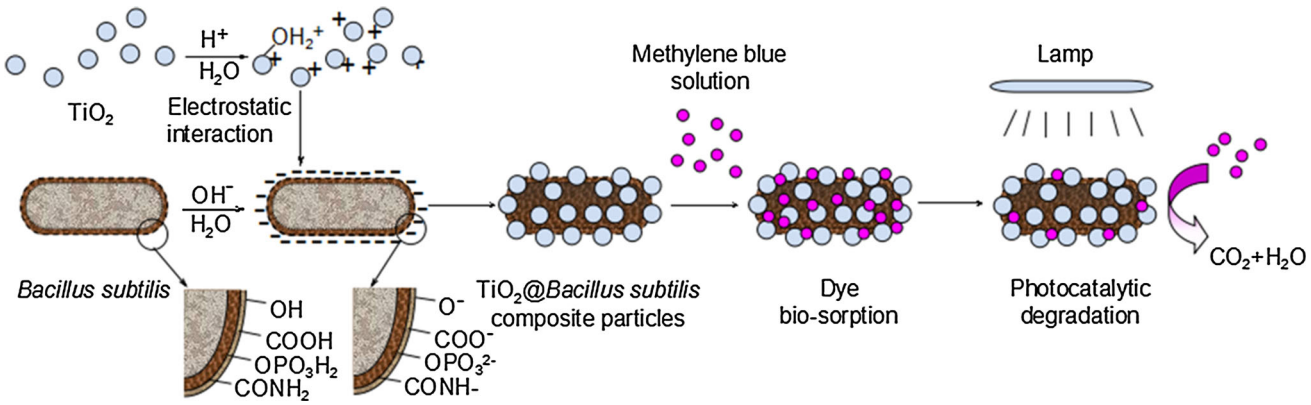

Keywords Self-assembly · Photocatalysis · Degradation · Biotemplate · Biosorption

1 Introduction

In recent years, microbial cells as biotemplates have attracted burgeoning interests in a new research field of micro-nano materials synthesis, due to the major advantages, including abundant resources, easy accessibility, renewable and environmentally friendly materials, easy to remove, special and highly repetitive configurations and so on [1–3]. For example, nano-capsid, *Escherichia coli*, *Deinococcus radiodurans* and *yeast* cells have been used as biotemplates in the fabrication of micro-nano materials [4–7]. Especially, the photocatalytic materials synthesized by microbial cell templates have represented excellent comprehensive properties. Bo Bai et al. [8] reported the synthesis of novel TiO_2@*yeast* composite particles with raspberry-like morphology by a simple single-step electrostatic process. The TiO_2@*yeast* composite particles with selective bio-sorption and photocatalytic function have been applied into the decolourization of methylene blue and shown great effectiveness. Han Zhou et al. [9, 10]

✉ Chao Yan
15249264959@163.com

[1] College of Environmental Science and Engineering, Chang'an University, Xi'an 710054, People's Republic of China

[2] Northwest Plateau Institute of Biology, Chinese Academy of Sciences, Xining 810001, People's Republic of China

developed a novel and general bacteria-based bottom-up approach to synthesize biomorphic porous PbS and ZnS hollow nanostructures using *Streptococcus thermophilus* and *Lactobacillus bulgaricus* as morph-biotemplates.

Bacillus subtilis, known as a member of the genus *Bacillus*, is an extremely common bacterium found in soil, water, air, and decomposing plant matter [11, 12]. Due to abundance and the special physicochemical/biological properties [13], *B. subtilis* exhibits an ideal candidate as a microbial cell template for the formation of micro-nano photocatalytic composite materials. To be specific, *B. subtilis* cells are rod-shaped around 2 μm in length and 400 nm in width with a rigid cell wall structure [14]. The cell wall, comprised virtually of 46 % peptidoglycan and 54 % teichoic acids, is a peritrichous structure with abundant hydroxyl (–OH), acylamino ($–CONH_2$), carboxyl (–COOH), amino ($–NH_2$) and phosphate ($–OPO_3H_2$) functional groups [15, 16]. Therefore, such coexistence of peritrichous structure and the hydrophilic functional groups in the framework of *B. subtilis* cell wall provides plentiful absorption sites [17] and excellent absorbility [18, 19], which makes a good reason to utilize *B. subtilis* as a biotemplate to synthesise micro-nano photocatalytic composite materials. Moreover, the excellent suspension, dispersibility, easy availability and pretreatment of natural *B. subtilis* support the application as well. However, there are no articles on the facilitation of micro-nano photocatalytic composite materials with *B. subtilis* cells and TiO_2 nanoparticles.

In the present study, we report the manufacture of novel TiO_2@*Bacillus subtilis* composite particles using *B. subtilis* cells as biotemplates via a simple single-step electrostatic process. The product maintained the shape of the primitive *B. subtilis* cores and simultaneously integrated the particular natures of each participator (*i.e.*, good suspensibility, dispersibility, large contact area and bio-sorption capacity from *B. subtilis* cells and photocatalytic activity from TiO_2 nanoparticles). The structures of samples were characterized and the formation mechanism was proposed. The bio-sorptions and photocatalytic degradations of rhodamine B (RB) by composite materials were investigated further.

2 Experimental Section

2.1 Preparation of TiO_2@*Bacillus subtilis* Composite Particles

The preparation of TiO_2@*Bacillus subtilis* composite particles was based on self-assembly driven heterocoagulation. Briefly, 350 mg spores *B. subtilis* cell powders (air-dried) were suspended in 100 ml distilled water and the mixed solution was adjusted to pH 9–10 approximately by adding drop-wise sodium hydroxide solution. In a separate vessel, 50.0 mg TiO_2 nanoparticles (AEROXIDE-TiO_2 Degussa P25, primary particle size, 20–30 nm by TEM; specific surface area 52 m^2/g by BET; composition 78 % anatase and 22 % rutile by X-ray diffraction) were dispersed in 100 ml distilled water and the TiO_2 suspension was adjusted to pH 3–4 by adding drop-wise sulphuric acid solution. Next, the two suspensions were simultaneously sonicated in an ultrasonic bath for 10 min to facilitate de-aggregation of the particles and then respectively centrifuged to obtain alkali-treated *B. subtilis* cells and acid-treated TiO_2 nanoparticles at a rate of 5000 revolutions per minute. After that, *B. subtilis* cells and TiO_2 nanoparticles were re-dispersed again in 75 ml distilled water respectively and mixed for 1.0 h by magnetic stirring to promote the electrostatic attachment of TiO_2 nanoparticles onto the surface *B. subtilis* cell wall. The resultant pH was approximately 4.5, which promoted self-assembly of TiO_2 nanoparticles onto *B. subtilis* cell wall. The above mixture was left for 2.0 h at ambient temperature and pressure to form the TiO_2@*Bacillus subtilis* composite particles. The resulting particles were collected by centrifugation from the mixture, followed by two cycles of distilled water and ethanol rinsing. The obtained TiO_2@*Bacillus subtilis* composite particles were dried in air at 60 °C for 5 h and stored in a sealed bottle at ambient temperature for further use.

2.2 Characterization

The morphology of primitive *B. subtilis* and final TiO_2@*Bacillus subtilis* microparticles were studied using Hitachi S4800 scanning electron microscopy (SEM) on the double sided adhesive conductive carbon tape with thin layers of platinum sputtered onto the samples before imaging. The detailed composition characterization of the TiO_2@*Bacillus subtilis* composite particles was carried out with energy-dispersive spectroscopy (EDS) analysis. An X-ray diffraction (XRD) study was carried out using Cu Kα radiation ($\lambda = 0.15418$ nm) at a scanning rate of 0.02° per min. FTIR spectra of the samples were recorded with a Nicolet FT-IR spectrometer using a KBr disc containing 10 % of each finely ground sample in the range of 400–4000 cm^{-1}. The supernatants of solutions were analyzed on a UV–Vis spectrophotometer (TU 4100) to determine the residual RB concentration ($\lambda_{max} = 552$ nm).

2.3 Decolourization of RB

The TiO_2@*Bacillus subtilis* composite particles were applied to degrade the concentration of the cationic dye,

rhodamine B, to further investigate the TiO_2@*Bacillus subtilis* removal effeciency of water contaminants. The bio-absorptive capacity and photocatalytic activities of TiO_2, bare *B. subtilis* and TiO_2@*Bacillus subtilis* composite particles were evaluated by the following experimental procedures: 200 mg per sample was dispersed in 100 mL RB solution (140 mg L^{-1} initially). The suspensions were magnetically stirred in the dark for 90 min to establish absorption–desorption equilibrium respectively. Then the suspensions were treated by UV irradiation, which was produced by a 500 W high pressure Hg lamp placed 8 cm above the beakers. Before and after UV irradiation, 4 mL suspension of each mixture was collected every 30 min and centrifuged to separate the catalyst from the suspension. And the supernatants were analyzed colorimetrically on a UV–visible spectrophotometer (TU-4100) to determine the concentrations of the residual RB. The bio-sorption and photoreduction ratio (%) could be calculated from the following equation:

$$\eta_1 = \frac{c_s - c_o}{c_o} \times 100\% \quad (1)$$

$$\eta_2 = \frac{c_o - c_e}{c_o} \times 100\%, \quad (2)$$

where η_1, η_2 are bio-sorption and photoreduction ratios, c_s, c_o and c_e are concentrations of RB before adsorbing, before and after irradiation, respective.

3 Results and Discussion

Figure 1a–c shows the SEM images of naked *B. subtilis* and TiO_2@*Bacillus subtilis* composite particles. In Fig. 1a, the primitive *B. subtilis* cells were ordered rods with the length of around 1.3 ± 0.1 μm and width of 400 ± 50 nm. In Fig. 1b, The TiO_2@*Bacillus subtilis* composite particles maintained the shape of the primitive *B. subtilis* cores and possessed relatively good monodispersity. Due to the nanoparticles on the surface of *B. subtilis*, the composite particles were 1.4 ± 0.1 μm in length and 450 ± 50 nm in width. As can be seen in Fig. 1c, parts of the *B. subtilis* surface was covered with TiO_2 nanoparticles under high magnification, which roughened the surface of cell wall in comparison with primitive *B. subtilis*. Figure 1d presented the EDS analysis of TiO_2@*Bacillus subtilis* composite particles. Obviously, Ti element was observed on the cell wall surface, which provided an evidence of the existence of TiO_2 nanoparticles on the surface of the *B. subtilis* cells.

XRD spectra of the bare *B. subtilis*, TiO_2 nanoparticles and TiO_2@*Bacillus subtilis* composite particles were exhibited in Fig. 2. In Fig. 2a, the unconspicuous and broad peak around $2\theta = 20°$ was attributed to the amorphous phase of *B. subtilis*. The sharp diffraction peaks at 25.30°, 37.82°, 48.10°, 53.94°, 55.08°, 62.61°, 69.00°, 70.22° and 27.45°, 75.00° of the TiO_2@*Bacillus subtilis* composite particles (Fig. 2b) corresponded well with the reflections of

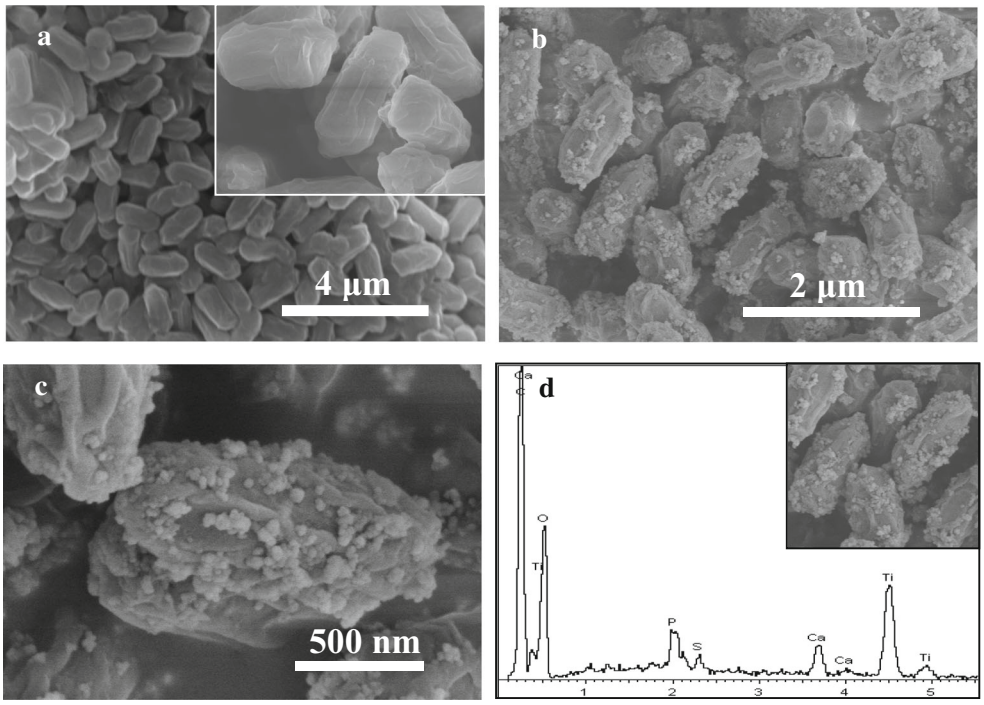

Fig. 1 SEM images of **a** naked *Bacillus subtilis*, **b** general observation of the TiO_2@*Bacillus subtilis* composite particles, **c** typically TiO_2@*Bacillus subtilis* composite particles observed under high magnification, and EDS spectrum of the TiO_2@*Bacillus subtilis* composite particles

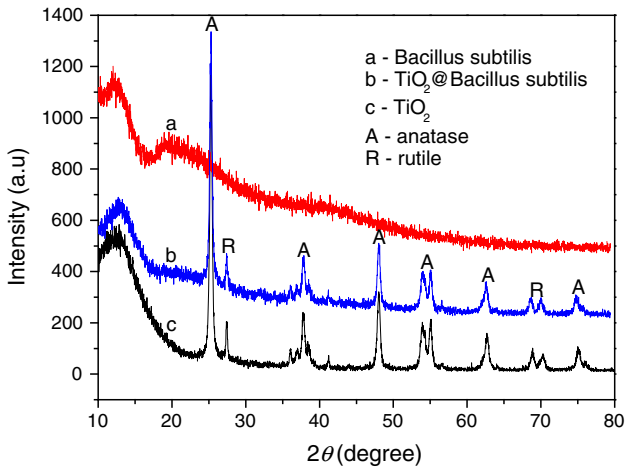

Fig. 2 XRD patterns of (*a*) the original *Bacillus subtilis*, (*b*)TiO_2@-*Bacillus subtilis* composite particles and (*c*) TiO_2 nanoparticles

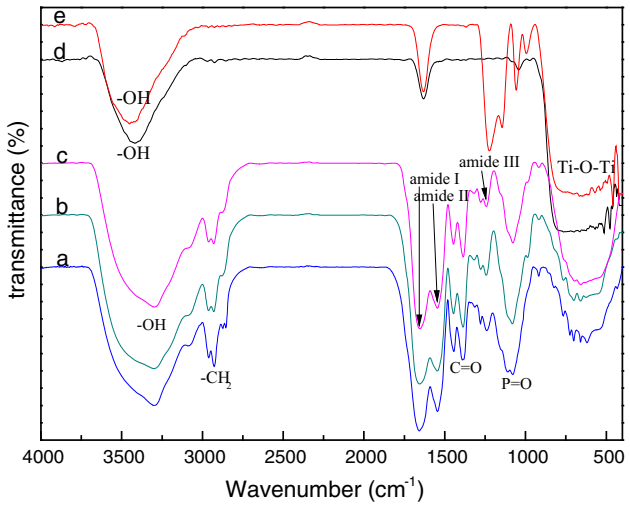

Fig. 3 FT-IR spectra of (*a*) the original *Bacillus subtilis*, (*b*) *Bacillus subtilis* treated by NaOH solution, (*c*) TiO_2@*Bacillus subtilis* composite particles, (*d*) pristine TiO_2 and (*e*) TiO_2 nanoparticles treated by H_2SO_4 solution

anatase and rurile phase respectively (JCPDS NO. 21-1272), which were similar to the characteristic peaks of TiO_2 nanoparticles (Fig. 2c). The intensity change of TiO_2@*Bacillus subtilis* composite particles (Fig. 2b) around $2\theta = 20°$ was different with that of TiO_2 nanoparticles (Fig. 2c), due to the amorphous structure of *B. subtilis*. The results above demonstrated that TiO_2 nanoparticles attached onto the *B. subtilis* cell wall and the crystalline phase of TiO_2 nanoparticles remained unchanged.

Figure 3 exhibited the FT-IR spectra of original *B. subtilis*, pristine TiO_2, TiO_2@*Bacillus subtilis* composite particles, and their intermediate synthesis stages. In Fig. 3a, the broad peaks of *B. subtilis* at 3298, 2927, 2854, 1654, 1544, 1380, 1240 and 1078 cm^{-1} were assigned to the stretching vibration of O–H stretching vibration, symmetric and asymmetric stretching vibration of methylene, amide I, amide II, C=O stretching vibration, amide III and P=O stretching vibration, respectively [20, 21]. The characteristic peaks of alkali-treated *B. subtilis* cells in Fig. 3b were similar to that of *B. subtilis* cells. In Fig. 3d, e, the intense peaks at 3417 cm^{-1} (O–H stretching vibration) and 900–500 cm^{-1} (Ti–O–Ti) were both observed in pure TiO_2 and acid-treated TiO_2 nanoparticles. After self-assembly interaction of alkali-treated *B. subtilis* cells and acid-treated TiO_2 nanoparticles, as can be seen in Fig. 3c, the characteristic peaks of the *B. subtilis* composite particles at 1380 and 1240 cm^{-1} were shifted to 1386 and 1242 cm^{-1}, respectively. The vibration intensities of –OH bond became stronger, and that of amide III and O=P bonds became weaker in comparison to bare *B. subtilis* cells, suggesting that –OH, $–CONH_2$, $–COO^-$ and $–OPO_3^{2-}$ functional groups are major contributors for the anchoring of the TiO_2 nanoparticles. The peaks ranging from 1000 to 500 cm^{-1} were increased, due to Ti–O-Ti absorption typical of TiO_2 type phase, which indicated the successful fabrication of TiO_2@*Bacillus subtilis* composite particles. The results were in good agreement with XRD analysis.

Based on the above analysis, the possible formation mechanism of TiO_2@*Bacillus subtilis* composite particles synthesized by electrostatic self-assembly were proposed in Scheme 1. The materials with sufficiently high opposite zeta-potentials drove self-assembly via electrostatic interaction and achieved stable guest–host particles suspensions [22]. Specifically, the isoelectric point of the TiO_2 nanoparticles was approximately pI of 6.8 [23, 24]. When dissolved in water, there generated surface hydroxyl groups ($\equiv$Ti–OH) on TiO_2 nanoparticles and produced the positively charged surface ($\equiv Ti–OH_2^+$) after proton association or dissociation reaction in acid solution [8]. Below pH of 6.8, the TiO_2 nanoparticles were positively charged and there was a gradual increase of positively charged groups as the pH was lowered [8, 25, 26]. Similarly, the isoelectric point of the *B. subtilis* cells was about pI of 2.19 [27]. The complicated components of *B. subtilis* cell wall, including peptidoglycan, teichoic acids, etc., endowed the cell wall with abundant hydrophilic anionic groups, including OH^-, $–CONH^-$ and $–COO^-$, which provided ideal binding sites for the protonated hydroxyl groups. Therefore, it can be speculated that TiO_2 nanoparticles and *B. subtilis* cells have opposite zeta-potentials in the range of pH from 2.2 to 6.8. At pH of approximately 4.5, the electrostatic driving force reached a maximum to improve the self-assembly of TiO_2 nanoparticles onto *B. subtilis* cells. Futher low-temperature heating resulted in the formation of –O–O– bonds due to partial dehydration [28]. Hence, the mechanical stability and strength of adhesion were enhanced.

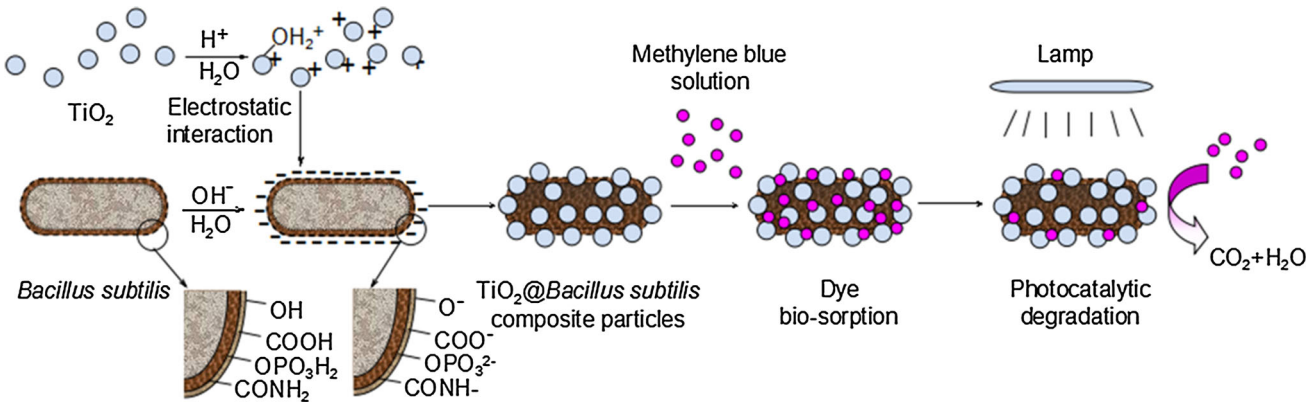

Scheme 1 Formation mechanisms of the TiO_2@*Bacillus subtilis* composite particles and the synergetic effect in the removal of dyes aqueous solution

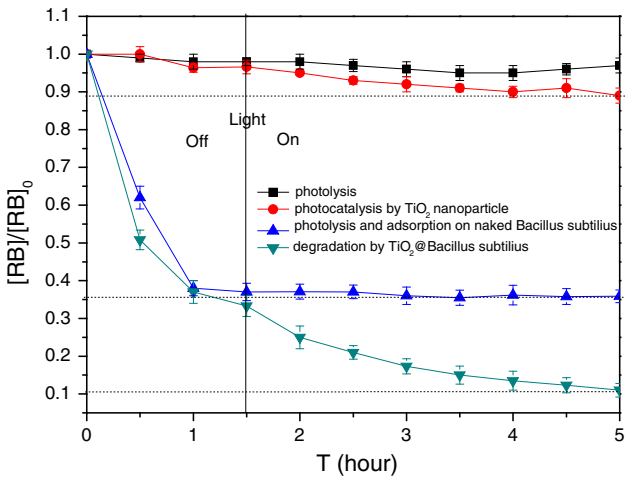

Fig. 4 Changes in relative concentration of RB due to photolysis, photocatalysis by TiO_2 nanoparticle, photolysis and adsorption on naked *Bacillus subtilis* and degradation by TiO_2@*Bacillus subtilis* composite particles. $[RB]_0 = 140$ mg L^{-1}

To further examine the application of TiO_2@*Bacillus subtilis* composite particles in the removal of water contaminants, the aqueous solution of RB, was taken as an example. As shown in Fig. 4, the bio-sorption and photocatalytic degradation of RB by pure *B. subtilis*, TiO_2 nanoparticles and TiO_2@*Bacillus subtilis* composite particles were performed respectively via the pretreatment of 1.5 h dark phase and the UV irradiation of 3.5 h. Clearly, the absorption–desorption equilibrium was established during the 1.5 h dark phase preceding the irradiation of the dyes solutions. Compared with *B. subtilis*, TiO_2@*Bacillus subtilis* composite particles exhibited more favourable bio-sorption capacity. The increase was assigned to the enhanced negatively charged surface by alkalization treatment, which facilitated the capture of the cationic RB dye through electrostatic attraction. The removal ratio of RB by *B. subtilis* was about 64 %, while the removal ratio of RB by TiO_2@*Bacillus subtilis* composite particles was approximately 89 %. The increase was attributed to combination of the bio-sorption ability of *B. subtilis* cells and photocatalytic activity of TiO_2 nanoparticles. What is more, the well suspension property and dispersibility, large contact area facilitate the bio-sorption capacity of TiO_2@*Bacillus subtilis* composite particles, which may provide TiO_2 nanoparticles with RB molecule for photocatalytic degradation on the surface of *B. subtilis* cells. In return, the photocatalytic degradation of RB molecule on the surface can refresh the bio-sorption capacity of TiO_2@*Bacillus subtilis* composite particles. These two mutually enhancing processes significantly increase the removal ratio of RB. All the results above suggested that TiO_2@*Bacillus subtilis* composite particles were effective for dye removal, due to the integrated combined properties originated from their hybrid components, such as well suspension property and dispersibility, large contact area, favourable bio-sorption capacity and photocatalytic activity.

4 Conclusions

In summary, we have successfully developed a simple, economical and friendly environmental route for the manufacture of TiO_2@*Bacillus subtilis* composite nanomaterials by a single-step strategy based on electrostatic interaction driving self-assembling heterocoagulation. The samples were characterized by SEM, EDS, XRD and FT-IR spectroscopy analyses. The possible formation mechanism of TiO_2@*Bacillus subtilis* composite particles was proposed. The effectiveness of the TiO_2@*Bacillus subtilis* composite particles for the removal of water contaminants was investigated by decolourizing RB and the removal ratio was approximately 89 %. The obtained materials with biotemplates possess integrated combined

properties of well suspension and dispersibility, large contact area, favourable bio-sorption capacity and photocatalytic activity and have potential applications in the treatment of different waste water.

Acknowledgments This work was financially supported by the Fundamental Research Funds for the Central Universities of China (2014G3292007).

References

1. Bai B, Guan WS, Li ZY (2010) Mater Res Bull 46:26
2. Gunaseker V, Divya B, Vijaykrishnan J (2013) J Sol Gel Sci Technol 68:60
3. Dou LL, Gao LS, Yang XH (2012) J Hazard Mater 203:363
4. Liu C, Chung SH, Jin QL, Sutton A, Yan F, Hoffmann A, Kay BK, Bader SD, Makowski L, Chen LH (2006) J Magn Magn Mater 302:47
5. Mogul R, Getz Kell JJ, Cable ML, Hebard AF (2006) Mater Lett 60:19
6. Zhou WJ, He W, Ma JY, Wang MT, Zhang XD, Yan SP, Tian XY, Sun XN, Han XX (2009) Mat Sci Eng C 29:1893
7. Zhou WJ, He W, Zhang XD, Zhao HS, Li ZM, Yan SP, Tian XY, Sun XN, Han XX (2009) Mater Chem Phys 116:319
8. Bai B, Quici N, Li Z (2011) Chem Eng J 170:451
9. Zhou H, Fan TX, Han T, Li XF, Ding J, Zhang D, Guo QX, Ogawa H (2009) Nanotechnology 20:1
10. Zhou H, Fan TX, Ding J, Zhang D, Guo QX (2012) Opt Lett 20:340
11. Filip Z, Herrmann S, Kubat J (2004) Microbiol Res 159:257
12. Boer AS, Diderichsen B (1991) Appl Microbiol Biot 36:1
13. Ayla A, Cavus A, Bulut Y, baysal Z, Aytekin C (2013) Desalin Water Treat 51:40
14. Perez AR, Abanes-De Mello A, Pogliano K (2000) J Bacteriol 182:1096
15. Graham LL, Beveridge TJ (1994) J Bacteriol 176:1413
16. Ashtari K, Fasihi J, Mollania N, Khajeh K (2014) Mater Res Bull 50:348
17. Beveridge TJ, Murray RG (1980) J Bacteriol 141:876
18. Beveridge TJ, Murray RG (1976) J Bacteriol 127:1502
19. Boyanov ML, Kelly SD, Kemner KM, Bunker BA, Fein JB, Fowle DA (2003) Geochim Cosmochim Acta 67:3299
20. Gnanasambandam R, Protor A (2000) Food Chem 68:327
21. Pan JH, Ge XP, Liu RX, Tang HX (2006) Colloid Surf B 52:89
22. Dong HY, Lu K (2009) J Appl Ceram Technol 6:216
23. Barakat MA (2005) J Colloid Interface Sci 291:345
24. Veronovski N, Andreozzi P, La Mesa C, Sfiligoj-Smole M (2010) Surf Coat Technol 204:1445
25. Mercier-Bonin M, Ouazzani K, Schmitz P, Lorthois S (2004) J Colloid Interf Sci 271:342
26. Mozes N, Marchal F, Hermesse MP, van Haecht JL, Reuliaux L, Leonard AJ, Rouxhet PG (1987) Biotechnol Bioeng 30:439
27. Harris JO, Harden VP (1952) J Bacteriol 65:198
28. Turov VV, Gunko VM, Bogatyrev VM, Zarko VI, Gorbik SP, Pakhlov EM, Leboda R, Shulga OV, Chuiko AA (2005) J Colloid Interf Sci 283:329